

High-molar-mass Branched Poly[oxymethylene-oligo(oxyethylene)] for use in Polymer Electrolytes

Yan Pang,^{*a} Shao-Min Mai,^a Ke-Yong Huang,^a Yun-Zhu Luo,^a Jane H. Thatcher,^b Robert A. Colley,^b Christian V. Nicholas^b and Colin Booth^b

^a Department of Applied Chemistry, Shenzhen University, Shenzhen, Guangdong Province, People's Republic of China

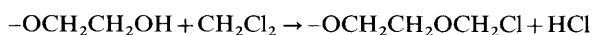
^b Manchester Polymer Centre and Department of Chemistry, University of Manchester, Manchester, UK M13 9PL

High-molar-mass poly[oxymethylene-oligo(oxyethylene)] (POMOE, oxymethylene-linked PEG400) was prepared by inclusion of a multifunctional alcohol in the polycondensation recipe. Approximate values of the critical concentration for gelation were determined. Branching in samples prepared at lower-than-critical concentrations was confirmed by comparison of molar masses determined by gel-permeation chromatography and static light scattering. Melt flow indices confirmed an increase in viscosity. Differential scanning calorimetry and dynamic mechanical thermal analysis were used to determine glass-transition and melting temperatures of the polymers and of mixtures of the polymers with lithium perchlorate. Conductivities of polymer-salt mixtures were measured. Comparison of results for branched and linear polymers indicated no significant difference in properties, including conductivity, apart from a decrease in melt flow index.

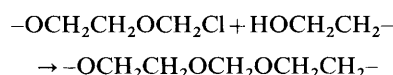
The use of ionically conducting polymer electrolytes based on lithium salts and high-molar-mass poly(oxyethylene) (POE) for construction of thin-film solid-state storage batteries was first proposed in 1978, but the unplasticised POE-based electrolytes then available had low conductivities at ambient temperatures (e.g., $\sigma < 10^{-7} \text{ S cm}^{-1}$ at 25°C).¹ Since that time, a number of polymer-salt systems with relatively high ambient-temperature conductivities ($\sigma < 10^{-5}$ – $10^{-4} \text{ S cm}^{-1}$ at 25°C) have been developed and applied. The situation has been thoroughly reviewed.^{2–5} One polymer used in this way is poly[oxymethylene-oligo(oxyethylene)], (POMOE).^{6–8} The repeat unit is $-\text{OCH}_2(\text{OCH}_2\text{OCH}_2)_n-$ where n , an average value over a narrow distribution of oxyethylene sequence lengths, is typically in the range 4–20. Starting from polyethylene glycol 400 (PEG400, $n \approx 9.1$), polymers of number-average molar mass in the range 50 000–150 000 g mol^{-1} have been prepared, corresponding to chains containing on average 100–300 repeat units. The oxymethylene groups that link the oxyethylene sequences disrupt the crystallinity. With a suitably chosen value of n these polymers can be non-crystalline at room temperature, and all have low glass transition temperatures, i.e., $T_g \approx -65^\circ\text{C}$.

In common with other elastomers with flexible chains (e.g., polydimethylsiloxanes, polyphosphazenes), non-crystalline POMOE is a soft rubber and is subject to creep. The present work was directed towards increasing the bulk viscosity of the polymer. The method described below was to incorporate a low-molar-mass polyfunctional alcohol into the polymerisation recipe to promote long-chain branching and to increase the molar mass. It was expected that the local environment in the polymer would be unchanged by long-chain branching and so, since the conductivity of a polymer electrolyte depends on local viscosity (segmental mobility) rather than bulk viscosity, it was expected that the conductivity would not differ significantly between polymer electrolytes incorporating linear and branched forms of the polymer. Indeed this was the experience of Sloop *et al.*⁹ who subjected POMOE-based polymer electrolytes to UV-irradiation and found no significant change in conductivity with limited cross-linking.

The polymerisation reaction in the presence of excess KOH proceeds through formation of the chloroether



followed by very rapid reaction of the chloroether with a second hydroxy group to form an oxymethylene link



Because of the extreme difference in reactivities of the chloromethylene and chloroether groups, the polymerisation proceeds effectively as an RA_2 self-condensation, yielding high molar mass products without the need for balancing the concentrations of reagents, as is necessary to achieve high molar masses in conventional $\text{RA}_2 + \text{RB}_2$ polycondensation.¹⁰

The inclusion of a multifunctional alcohol, such as trimethylolpropane [TMP; 2,2-bis(hydroxymethyl)butan-1-ol, $\text{CH}_3\text{CH}_2\text{C}(\text{CH}_2\text{OH})_3$], converts the reaction into an $\text{RA}_2 + \text{RA}_f$ polycondensation (where f is the functionality of the alcohol). The conditions for gel formation in such reactions have been defined.¹¹ If α is the probability that a sequence starting from a branch point ends in a branch point regardless of the sequence length, if p is the probability that an A group has reacted to form polymer, and if ρ is the mole fraction of A groups in RA_f molecules in the initial mix, then

$$\alpha = \frac{p\rho}{1 - p(1 - \rho)}$$

A value for p can be estimated from the number-average chain length (x_n , degree of polymerisation) obtained in an RA_2 polymerisation carried out under comparable conditions by application of the Carothers equation¹⁰

$$p = 1 - \frac{1}{x_n}$$

A chain length of $x_n \approx 200$, typical of a PEG400 polymerisation, would mean $p \approx 0.995$. For trifunctional branching ($f=3$), the critical value of α for gelation is $\alpha_c = 0.5$. Hence gelation would be expected if the mole fraction of RA_3 in the initial mix exceeded a critical value of $\rho_c = 0.005$. For tetrafunctional branching ($f=4$) gelation under the same conditions requires $\alpha_c = 0.333$ and $\rho_c \approx 0.0025$.

These calculations, which assume no ring formation, provided a semiquantitative guide in designing the polycondensations described below. The branching agents used were:

glycerol (GLY), $\text{CH}_2(\text{OH})\text{CH}(\text{OH})\text{CH}_2(\text{OH})$; TMP, $\text{CH}_3\text{CH}_2\text{C}(\text{CH}_2\text{OH})_2\text{CH}_2\text{OH}$; and pentaerythritol [PET; 2,2-bis(hydroxymethyl)propane-1,3-diol, $\text{C}(\text{CH}_2\text{OH})_4$]. The notation used for the polymers indicates the PEG and the type and amount of branching agent used, e.g., 400-GLY-2.0 denotes a polymer prepared from PEG400 ($M_n = 400 \text{ g mol}^{-1}$) and branched by use of 2.0 mol% glycerol. Linear polymer (no branching agent) is denoted 400-L. The thermal, dynamic-mechanical-thermal, and flow properties of the polymers were determined, as were the conductivities of solutions of lithium perchlorate in selected samples.

Experimental

Preparation and Characterisation of Polymers

Polyethylene glycol (PEG400) was dried under vacuum (10^{-3} mmHg) at room temperature for 24 h, and dichloromethane was purified by distillation. Samples of linear POMOE were prepared by reacting PEG400 with excess dichloromethane in the presence of excess finely powdered KOH. For example, finely ground potassium hydroxide (55 g) was mixed with dichloromethane (50 cm^3) under nitrogen at room temperature in a resin kettle equipped with a condenser. To this was added PEG400 (51.0 g), and the whole was stirred until the viscosity prohibited further stirring (ca. 1 h). The polymeric mass was allowed to stand under nitrogen for a further 16 h, after which it was divided and dissolved in additional dichloromethane. The resulting solution was filtered through diatomaceous earth, and the rubbery polymer was isolated by rotary evaporation before final drying on a vacuum line and storage at low temperature in a refrigerator.

Branched polymers were prepared in a similar way, but with inclusion of small quantities of the branching agent. In each case the amount of branching agent used was varied in order to locate the gel point. Because values of p for production of high polymer were well in excess of 0.99, the reaction was very sensitive to minor variations in conditions and in purities of reagents, which resulted in variation of the gel point. Consequently, limited ranges of values were obtained for the critical concentrations in each case. These values of ρ_c , and corresponding values of the mol% branching agent, are set out in Table 1. The values found for TMP and PET were in fair agreement with expectation. The much higher values of ρ_c found for glycerol reflect the low reactivity of its secondary hydroxy group.¹¹ The branched polymers described below were prepared using concentrations of the branching agents below the critical values (see Table 2).

^{13}C NMR was used as described earlier¹² to verify the overall chain structure of the polymers. Low-intensity resonances associated with the residues of the branching agents were not quantified. In keeping with the method used for preparation of the polymers,⁸ only very small fractions of low-molar-mass cyclic polymers were detected by GPC (see below), and separation of chains from rings (e.g., by precipitation fractionation^{8,12}) was not carried out. Residual potassium levels, detected by elemental analysis, were invariably $<0.1 \text{ wt.}\%$.

Preparation of Polymer-Salt Mixtures

Acetonitrile (Aldrich, 99%) was freshly distilled and stored over activated type-4A molecular sieve. Lithium perchlorate (reagent grade, Aldrich) was dried under vacuum before use (10^{-3} mmHg , 50°C , 2 days) and stored under anhydrous conditions. To prepare the films, samples of POMOE (ca. 0.1 g) were extensively dried under vacuum (room temperature), mixed with dry LiClO_4 and dry acetonitrile (5 cm^3) under dry nitrogen, and allowed to dissolve for several hours. After shaking, solutions were transferred onto poly(tetrafluoroethylene) plates under a dry nitrogen flow at room temperature to allow the solvent to evaporate. The polymer electrolyte films so formed were thoroughly dried under vacuum (2 days, room temperature) before storage under dry conditions at low temperature. Mole ratios of oxygen to metal were calculated taking into account all oxygen atoms.

Gel-permeation Chromatography

The analytical GPC systems comprised three columns, each 30 cm long packed with μ -Styragel (500, 10^4 , 10^6 \AA nominal pore size) and a differential refractometer detector (Knauer High Temperature). The eluent was DMA (*N,N*-dimethylacetamide) at 65°C , pumped at $1 \text{ cm}^3 \text{ min}^{-1}$. Sample solutions (concentration 5 g dm^{-3}) were injected *via* a 0.1 mm^3 loop. Calibration was with linear poly(oxyethylene) standards.

Static Light Scattering

Static light scattering (SLS) measurements were made by means of an Otsuka DLS-700 instrument with vertically polarised incident light from a 5 mW He-Ne laser ($\lambda = 632 \text{ nm}$). Polymer solutions in prefiltered methanol at 30°C were further clarified by passage through $0.22 \mu\text{m}$ filters (Millipore, Millex-GS). Solutions of samples with very high

Table 1 Critical parameters for gelation

branching agent	ρ_c (expected) ^a	ρ_c (experiment) ^a	mol% (experiment) ^b
GLY	0.005	0.06–0.075	4–5
TMP	0.005	0.003–0.006	0.2–0.4
PET	0.0025	0.003–0.005	0.15–0.25

^a ρ_c = critical fraction for gelation, either calculated (expected) assuming $p = 0.995$, or observed (experiment). ^b mol% = corresponding critical mol% of branching agent in the mixture.

Table 2 Polymers prepared with and without branching agents, characterisation by GPC, SLS and MFI

polymer	mol% branching agent	$M_{pk}/\text{g mol}^{-1}$ (GPC)	$M_w/\text{g mol}^{-1}$ (SLS)	M_w/M_{pk}	$(\text{MFI})^{-1}/\text{min g}^{-1}$
400-L	0	2.3×10^5	3.7×10^5	1.6	1.3
400-GLY	3.2	1.8×10^5	4.6×10^5	2.6	—
400-TMP	0.15	1.0×10^5	2.1×10^5	2.1	1.7
400-TMP	0.20	0.65×10^5	1.7×10^5	2.6	—
400-PET	0.20	3.8×10^5	1.2×10^6	3.2	6.3

molar masses were difficult to filter. Filtration through 0.45 μm filters was possible, but filtration through finer filters was extremely slow. However, comparison of scattering intensities from filtered and unfiltered solutions generally showed only small differences, and this was taken to mean that the samples were optically clean as prepared.

Intensities of scattered light were measured over a range of angles from 45° to 135°. The customary double extrapolation (concentration and angle) of the light scattering function was used to determine M_w . The refractive index increment at 30 °C, required for calculation of M_w , was measured by means of a precision Abbé refractometer (Bellingham and Stanley): *i.e.*, $dn/dc = 0.141 \text{ cm}^3 \text{ g}^{-1}$.

Melt Flow Index

Melt flow indices (MFI) were measured by means of a Ray-Ran Melt Flow Indexer equipped with a 4.8 mm bore die. The temperature was maintained at 80 °C. A polymer sample was tamped into the barrel (9.5 mm i.d.) before fitting the piston. After 5 min to allow temperature equilibration, a 21.6 kg weight was applied and the MFI (g min^{-1}) was determined as the piston moved between two marked positions.

Dynamic–Mechanical–Thermal Analysis

Dynamic mechanical thermal analysis (DMTA) was carried out by means of a Polymer Laboratories MKII DMTA used in the shear-sandwich mode. Samples were cooled to -100°C , and measurements of complex modulus (G^*) were made at frequencies in the range 0.3–30 Hz whilst heating from -50 to $+100^\circ\text{C}$ at 1 K min^{-1} . Samples were clamped at low temperatures to counteract shrinkage, but not further adjusted during heating, which meant that values of $\log(G^*/\text{Pa})$ at the higher temperatures were known only to ± 0.3 , as judged by replicate measurements. At low temperatures, the modulus approached the limit of measurement for the instrument in the geometry used (*i.e.*, $G^* \approx 10^8 \text{ Pa}$) which meant that T_g could not be defined by our technique.

Differential Scanning Calorimetry

A Perkin-Elmer DSC-4 was used. Dry samples (4–8 mg) were sealed into aluminium pans under dry nitrogen and cooled rapidly, in the calorimeter, to -100°C . Starting at this temperature, each sample was heated at $+10 \text{ K min}^{-1}$ to 100°C . The samples were then cooled rapidly (quenched) from $+100^\circ\text{C}$ to -100°C and then re-heated at $+10 \text{ K min}^{-1}$. Melting and glass-transition temperatures were obtained from the DSC curves as the temperature at the peak and the mid-point, respectively. The correction for thermal lag at the heating rate used was -2 K , as determined by experiments on melting point standards at various heating rates. Values of T_g were similarly corrected by determining mid-point values on heating and cooling at 10 K min^{-1} and assuming that the mean of the two values approximated the true value: this correction was also -2 K at a heating rate of 10 K min^{-1} . Calibration of the power and temperature scales was initially with pure indium, the temperature scale being checked by melting organic standards.

Conductivity

Conductivities of solutions of LiClO_4 in selected polymers were determined over a range of temperatures (20–80 °C) by ac impedance spectroscopy. A Schlumberger Model 1260 impedance/gain phase analyser was used over a frequency

range 5–15 MHz. The resistance was obtained as the point where the semicircle and the extrapolation of the inclined spike cut the real impedance axis. A dry film, prepared as described above, was sandwiched between two polished brass electrodes and held in place by springs within a cylindrical glass cell. This operation took place under a dry nitrogen atmosphere. The assembled cell, maintained under a slight positive pressure of nitrogen, was placed in a temperature-controlled oven (Buchi Model TO-51, $\pm 1^\circ\text{C}$). The temperature (measured by a thermocouple to $\pm 0.1^\circ\text{C}$) was raised to 80 °C and conductivities were determined at several temperatures on cooling from 80 to 20 °C. About 20 min was allowed for thermal equilibration at each temperature of measurement. Film thickness was monitored at all times by means of a travelling microscope ($\pm 0.001 \text{ cm}$).

Results and Discussion

Characterisation of Polymers

All polymers were examined by GPC, and some were subjected to more detailed examination by SLS and MFI, see Table 2.

GPC

Since calibration was against POE standards, the molar masses obtained by GPC were 'as if linear poly(oxyethylene)'. As might be expected, considering the dependence of GPC elution volume on molecular size rather than molecular mass, these results did not in themselves reflect branching in the products, since high molar masses caused by branching were compensated by more compact dimensions. Typically, molar masses taken from the calibration at points corresponding to the peaks of the GPC curves fell in the range $M_{pk} = 1 \times 10^5$ – $3 \times 10^5 \text{ g mol}^{-1}$ irrespective of the method of preparation.

SLS

Weight-average molar masses from SLS are given in Table 2. As expected, values of M_w from SLS were higher than values of M_{pk} from GPC. Given the experimental uncertainties in the two methods (each at least $\pm 10\%$), the ratio $M_w/M_{pk} \approx 1.6$ obtained for the linear polymers (400-L in Table 2) was much as expected, since a linear polymer with the 'most probable' molar-mass distribution (as expected for a polycondensation) would have M_w higher than M_{pk} by about $\sqrt{2}$. Of the branched polymers listed in Table 2, values of $M_w/M_{pk} > 2$ indicate a significant degree of branching, with polymer 400-PET-0.20 ($M_w/M_{pk} > 3$) somewhat more branched. Values of $M_w/M_{pk} > 10$ ($M_w \rightarrow 10^7 \text{ g mol}^{-1}$) were measured for samples polymerised near the gel point but, because of difficulties in filtration, the characterisation could not be considered reliable. The samples studied further all had M_w no higher than *ca.* 10^6 g mol^{-1} .

MFI

The MFI obtained for the samples, which were measured under various conditions of shear rate, could not be quantitatively correlated with zero-shear melt viscosity. Nevertheless the values of inverse MFI listed in Table 2 provide a second indicator of successful modification of the polymers. As can be seen, the values of $(\text{MFI})^{-1}$ obtained correlate reasonably well with the GPC/SLS results.

DMTA

DMTA curves (complex modulus G^* versus temperature) obtained for selected polymers are illustrated in Fig. 1. Because of the difficulty of keeping specimens dry in our equipment,

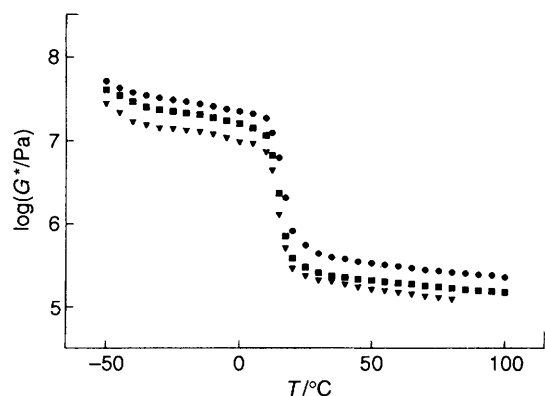


Fig. 1 DMTA curves of $\log(\text{complex modulus})$ versus temperature for (●) linear POMOE (400-L) and for branched POMOE: ■, 400-GLY-2.0; and ▼, 400-TMP-0.20. The estimated uncertainty in $\log G^*$ is ± 0.2 .

DMTA was not used for mixtures of polymers with LiClO_4 . Melting transitions at 15–17°C were clearly defined by the method. A gradual decrease in modulus as temperature was increased above the melting temperature was found in each case, indicative of a significant viscous component in G^* . Values of melting temperatures were not affected by the long-chain branching in the polymers. Within an uncertainty of approximately ± 0.2 in $\log G^*$, values of moduli were also identical for all samples studied. This uncertainty was due mainly to difficulty in clamping specimens in a reproducible way. Values of T_m and G^* representative of those found for all polymers investigated by DMTA are listed in Table 3 (row 1).

Thermal Analysis by DSC

Examples of DSC curves obtained for the polymers are shown in Fig. 2. The sequence of events on heating a polymer sample was: (i) glass transition in the range from -64 to -62°C; (ii) limited cold crystallisation in the range from -50 to -30°C; (iii) melting of unstable crystals in the range from -20 to 0°C; (iv) recrystallisation in the range from 0 to 10°C; and (v) melting in the range from 5 to 25°C. Characteristically, the final melting endotherm obtained for stored samples at a heating rate of 10 K min^{-1} showed evidence of recrystallisation effects: e.g., a high temperature shoulder (see Fig. 2). At slower heating rates, as a result of recrystallisation, the endotherm of the high melting component was resolved as the major peak, and after annealing the sample close to the melting temperature, only the peak of the high melting component remained in the DSC curve. These effects have been illustrated and discussed previously.⁸ Quenched samples gave similar DSC curves, sometimes with more prominent evidence of recrystallisation, see Fig. 2. Values of T_g and T_m (taken as that of the highest melting component) were not affected by branching (within experimental error), and values

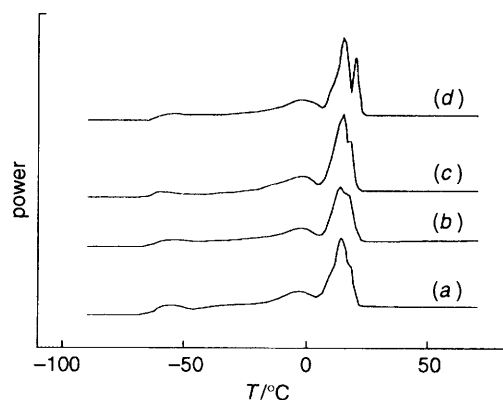


Fig. 2 DSC curves for samples of linear and branched samples of POMOE: stored samples 400-L (a), 400-GLY-2.0 (b) and 400-TMP-0.15 (c), and quenched sample 400-PET-0.20 (d). The heating rate was 10 K min^{-1} , and the temperature scale is uncorrected for thermal lag. The power scale is arbitrary, and baselines are adjusted.

representative of all polymers are given in Table 3 (row 1). The enthalpies of fusion obtained from the sum of peak areas between -50 and +30°C lie in the range $\Delta_f H = 45\text{--}60 \text{ J g}^{-1}$, irrespective of polymer type. The average value found for the various samples investigated by DSC (i.e., $\Delta_f H = 55 \text{ J g}^{-1}$) corresponded to a notional fractional crystallinity of $X \approx 0.30$, based on the thermodynamic enthalpy of fusion of poly(oxyethylene) $\Delta_f H^0 \approx 185 \text{ J g}^{-1}$ at $T \approx 15^\circ\text{C}$.¹³

Examples of DSC curves obtained for quenched polymer- LiClO_4 mixtures are illustrated in Fig. 3. No significant differences were found among the various polymers [see Fig. 3(a)]. As can be seen most clearly in Fig. 3(b), the effect of adding LiClO_4 was: (i) to increase the value of glass-transition temperature; (ii) to reduce the extent of crystallisation of the polymer at low salt concentrations ($\text{O}:\text{Li} \geq 25$), and to suppress crystallisation altogether (within the time scale of our experiments) at moderately-high salt concentration ($\text{O}:\text{Li} = 15$); and (iii) to decrease the rate of crystallisation on cooling in those samples which crystallised, and hence to increase the importance of cold crystallisation. Representative values of T_g , T_m and nominal extent of crystallinity (i.e., $X = \Delta_f H / \Delta_f H^0$) are listed in Table 3.

Similar DSC curves have been published previously for polymer electrolytes prepared from linear POMOE, and the effect of salt concentration on their melting and glass-transition temperatures has been fully discussed.^{14,15} The close conformity of the present to previous results is seen in the plot of T_g against mole ratio $\text{Li}:\text{O}$ shown in Fig. 4.

Conductivity

Representative Arrhenius plots of $\log \sigma$ (σ = conductivity) versus reciprocal temperature for the various systems at the same salt concentration ($\text{O}:\text{Li} \approx 25$) are shown in Fig. 5.

Table 3 Thermal analysis of linear and branched samples of POMOE with and without added LiClO_4 ^a

O:Li (LiClO_4)	$T_g/^\circ\text{C}$ (DSC, $\pm 2^\circ\text{C}$)	$T_m/^\circ\text{C}$ (DSC, $\pm 1^\circ\text{C}$)	X(%)	$T_m/^\circ\text{C}$ (DMTA, $\pm 1^\circ\text{C}$)	$\log(G^*/\text{Pa})$ (50°C, 1 Hz) (DMTA)
no salt	-64	15	25	16	5.5 ± 0.3
50	-58	15	14	—	—
35	-54	15	10	—	—
25	-50	14	3	—	—
15	-43	^b	^b	—	—

^a Row 1: results representative of all polymers. Rows 2–5: results for polymer 400-GLY-2.0. ^b No crystallinity.

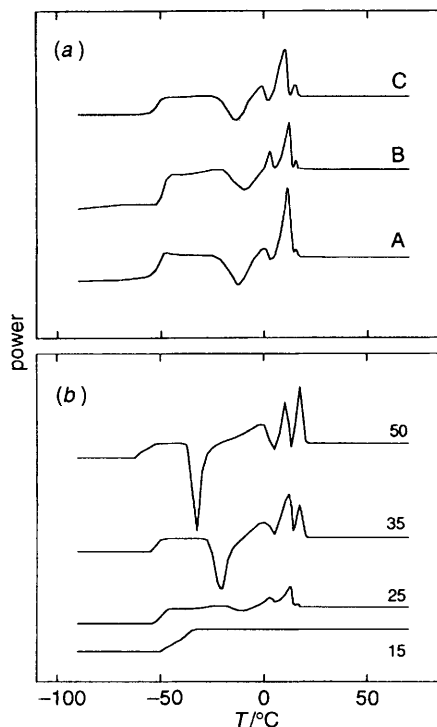


Fig. 3 DSC curves for mixtures of POMOE with LiClO_4 . (a) Branched and linear polymers mixed with LiClO_4 at mole ratio $\text{O}:\text{Li}=25$ (A, 400-L; B, 400-GLY-2.0; C, 400-PET-2.0). (b) Branched polymer 400-GLY-2.0 mixed with LiClO_4 at the mole ratios $\text{O}:\text{Li}$ indicated. The heating rate was 10 K min^{-1} , and the temperature scale is uncorrected for thermal lag. The power scales are arbitrary, and baselines were adjusted.

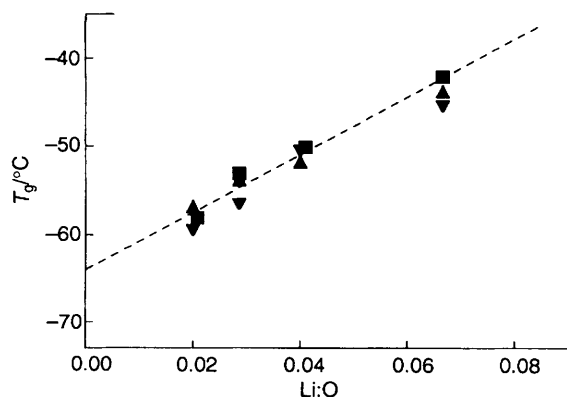


Fig. 4 Glass-transition temperature versus mole ratio $\text{O}:\text{Li}$ for branched POMOE mixed with LiClO_4 : (▲) 400-PET-0.2; (▼) 400-TMP-0.2; and (■) 400-GLY-2.0. The broken line represents results published previously¹⁴ for linear POMOE (400-L) mixed with LiClO_4 . The estimated uncertainty in T_g is $\pm 2^\circ\text{C}$.

Within the experimental uncertainty of results, the conductivities of the various systems were found to be identical.

Previously¹⁴ it was shown that the conductivities of mixtures of linear POMOE with LiClO_4 reached their maximum value at a mole ratio $\text{O}:\text{Li}$ of ca. 25. Similar results were obtained⁸ for mixtures of linear POMOE with LiCF_3SO_3 . This behaviour was explained as competition between an increase in concentration of charge carriers and an increase in local viscosity, the latter effect being monitored by the increase in the glass-transition temperature. The same behaviour (not illustrated) was found for the present systems.

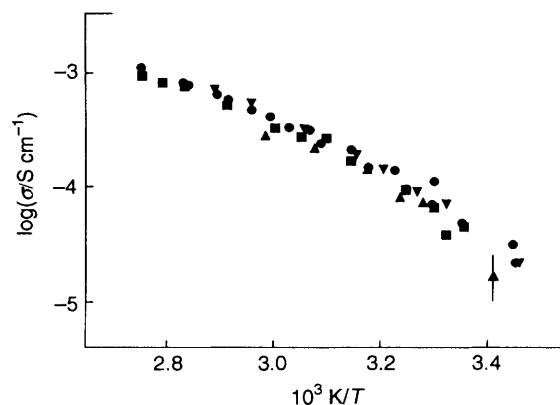


Fig. 5 Logarithm of conductivity ($\log \sigma$) versus inverse temperature for branched samples of POMOE mixed with LiClO_4 ($\text{O}:\text{Li} \approx 25$): (▲) 400-PET-0.2; (▼) 400-TMP-0.2; and (■) 400-GLY-2.0. Comparison is made with corresponding results (●) for linear POMOE (400-L) mixed with LiClO_4 at the same concentration. An uncertainty in the determination of σ of approximately $\pm 1 \times 10^{-5} \text{ S cm}^{-1}$ is shown for the lowest conductivity plotted. The same uncertainty at high conductivity is insignificant on the logarithmic scale.

Conclusions

It has been demonstrated that branched POMOE of high molar mass can be prepared by inclusion of a trifunctional or tetrafunctional branching agents in polymerisation. The thermal and dynamic-mechanical-thermal properties of the polymers, and the thermal and conduction properties of the polymer electrolytes, were unchanged by branching, but the bulk viscosities, in so far as they were monitored by melt flow index, were increased.

Dr. M. L. Clemens (Manchester Metropolitan University) kindly arranged for use of the melt flow indexer. Mr. A. Salmon and Mr. H. Bagshaw contributed through the Project Scheme of the Chemistry Department, University of Manchester. Mr. K. Nixon and Mr. M. Hart gave practical assistance with the GPC and DSC measurements. Financial support came from the British Council, the Science and Engineering Research Council and Trigon Packaging (UK) Ltd.

References

- 1 M. B. Armand, J. M. Chabagno and M. Duclot, *2nd International Conference on Solid Electrolytes*, St. Andrews, 1978, Abstracts, sect. 6.5.1.
- 2 *Polymer Electrolyte Reviews, Volumes 1 and 2*, ed. J. R. MacCallum and C. A. Vincent, Elsevier Applied Science, London, 1987 and 1989.
- 3 J. R. Owen, in *Comprehensive Polymer Science*, Vol. 2, ed. C. Booth and C. Price, Pergamon Press, Oxford, 1989, ch. 21.
- 4 P. G. Bruce and C. A. Vincent, *J. Chem. Soc., Faraday Trans.*, 1993, **89**, 3187.
- 5 F. M. Gray, *Solid Polymer Electrolytes*, VCH, New York, 1991.
- 6 J. R. Craven, R. H. Mobbs, C. Booth and J. R. M. Giles, *Makromol. Chem., Rapid Commun.*, 1986, **7**, 81.
- 7 C. Booth, C. V. Nicholas and D. J. Wilson in *Polymer Electrolyte Reviews, Volume 2*, ed. J. R. MacCallum and C. A. Vincent, Elsevier Applied Science, London, 1989, ch. 7.
- 8 C. V. Nicholas, D. J. Wilson, C. Booth and J. R. M. Giles, *Brit. Polym. J.*, 1988, **20**, 289.
- 9 S. E. Sloop, M. M. Lerner, T. S. Stephens, A. L. Tipton, D. G. Paull and J. D. Stenger-Smith, *J. Appl. Polym. Sci.*, 1994, **53**, 1563.
- 10 P. J. Flory, *Principles of Polymer Chemistry*, Cornell UP, Ithaca, NY, 1953, ch. 3.
- 11 P. J. Flory, *Principles of Polymer Chemistry*, Cornell UP, Ithaca, NY, 1953, ch. 9.

- 12 J. R. Craven, C. V. Nicholas, R. Webster, D. J. Wilson, R. H. Mobbs, G. A. Morris, F. Heatley, C. Booth and J. R. M. Giles, *Brit. Polym. J.*, 1987, **19**, 509.
- 13 C. Campbell, K. Viras, M. J. Richardson, A. J. Masters and C. Booth, *Makromol. Chem.*, 1993, **194**, 799.
- 14 S. Nagae, M. Nekoomanesh, C. Booth and J. R. Owen, *Solid State Ionics*, 1992, **53–56**, 1118.
- 15 J. H. Thatcher, K. Thanappapasr, S. Nagae, S-M. Mai, C. Booth and J. R. Owen, *J. Mater. Sci.*, 1994, **4**, 591.

Paper 5/00132C; Received 9th January, 1995